Paper 260

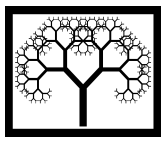

Proceedings of the Eleventh International Conference
on Computational Structures Technology,
B.H.V. Topping, (Editor),
Civil-Comp Press, Stirlingshire, Scotland

Spline-Based Hyperelasticity for Transversely Isotropic Incompressible Materials

M. Latorre and F.J. Montáns
Escuela Técnica Superior de Ingenieros Aeronáuticos
Universidad Politécnica de Madrid, Spain

Abstract

In this paper we present a spline-based hyperelastic model for incompressible transversely isotropic solids. The formulation is based on the Sussman-Bathe model for isotropic hyperelastic materials. We extend this model to transversely isotropic materials following a similar procedure. Our formulation is able to exactly represent the prescribed behavior for isotropic hyperelastic solids, recovering the Sussman-Bathe model, and to exactly or closely approximate the prescribed behavior for transversely isotropic solids. We have employed our formulation to predict, very accurately, the experimental results of Diani *et al.* for a transversely isotropic hyperelastic nonlinear material.

Keywords: hyperelasticity, splines, nonlinear elasticity, incompressible transversely isotropic materials, living tissues.

1 Introduction

Many real materials may be considered as transversely isotropic materials, as fiber composites [1], soils [2], some polymers [3] and specially living tissues [4] like bones [5], muscles as the myocardium [6], arteries [7] and even the skin [8]. Too often these materials are modeled as isotropic materials when large strain responses are to be analyzed. Large strain responses are obviously nonlinear, but frequently hyperelastic. Hyperelasticity implies that no energy is dissipated during closed cycles, or in other words, that stresses are a function of the strain state derived from a stored energy function (path independent). Such simple conceptual constraint is not easily implemented for any given material, characterized by some experimental data. The reason is that the necessary Riemann-type compatibility conditions are not easy to enforce for given experimental data, which are also sensible to some measurement errors. However, it

is essential to guarantee that those conditions are met in order to obtain no dissipation during elastic behavior, yielding mathematically and physically correct simulations (for example using finite elements).

The usual way to guarantee no dissipation without getting involved into solving the material compatibility equations is to directly prescribe a stored energy analytic function of the strains. This way, stresses are obtained by derivation of that stored energy function. The elastic (consistent) tangent, the elasticity tensor which is unique for each strain state, is obtained by second derivation of the stored energy function respect to the strains. Since it is impossible to experimentally determine the stored energy function, an explicit family of functions is formulated and assumed. This family of functions prescribes the "shape" of the stress-strain relation. Some material parameters are used in order to obtain a best fit to experimental data. Well known models widely available for isotropic materials are the Ogden model [9], the Mooney-Rivlin model [10][11], the Blatz and Ko model [12], the Arruda-Voyce model [13], etc. Many of these models are available in many commercial finite element codes. Models for anisotropic or transversely isotropic materials are more scarce, we may cite the model of Itskov and Aksel [14] or Holzapfel et al. [15]. Some of these models have been developed for specific materials, even though they are used for many more materials. The user must select the best model to fit the needs of the problem to be analyzed and then try to do the best to fit the experimental data for the material. Frequently, even though the global description may be captured, some details of the experimentally obtained behavior may be missed.

Therefore, what an engineer would like is to simply prescribe some (nonlinear but elastic) stress-strain data in a finite element program and to obtain the intended prescribed behavior, which accounts both for truly elasticity (nondissipative behavior) and for detailed stress-strain experimental behavior. In order to bridge this gap, Sussman and Bathe [16] developed a hyperelastic model for nonlinear isotropic materials based on a detailed splines interpolation of experimental data. With this model, the user prescribes some stress-strain data and a piecewise spline interpolation facilitates an analytical expression for the stresses which can derive from a stored energy function, even though the stored energy function needs not to be explicitly stated. The model exactly predicts the experimental behavior at the given stress-strain points. Since the stresses are derived from a strain energy function no dissipation takes place during cyclic loading.

However, the model developed by Sussman and Bathe is valid only for isotropic materials. As mentioned, many materials of interest are transversely isotropic. The purpose of the present paper is to present an extension of the model to transversely isotropic materials. For the isotropic case, the model of Sussman and Bathe is exactly recovered by our model.

In the first part of the paper we review some needed concepts for the formulation, introducing at the same time the notation of the paper. In the second part we comment on the procedure to obtain the model for given stress-strain data. Finally, we apply the explained concepts to predict the experimental behavior obtained by Diani et al. [17]

for a transversely isotropic material.

2 Spline-based interpolation

One of the basic ingredients is the spline-based interpolation of the experimental data. We use piecewise cubic splines between any two stress-strain points of the experimental data, say $(\tilde{\sigma}_i, \tilde{E}_i)$. The stress and strain measures we use are the generalized Kirchhoff stresses and the logarithmic strains. Hence, proper conversion of experimental data may be needed. The cubic interpolation spline $P(E)$ is a polynomial of up to third degree between any two points $\tilde{E}_i$ such that has the following properties

1. Satisfies the desired interpolation conditions on the experimental data, that is $P(\tilde{E}_i) = \tilde{\sigma}_i$ for all $i = 1, ..., n$, where n is the number of experimental points.

2. $P(E)$ is twice continuously differentiable in all the experimental range, i.e. in the domain $[\tilde{E}_1, \tilde{E}_n]$.

3. For *natural* splines, satisfies the boundary conditions $P''(\tilde{E}_1) = P''(\tilde{E}_n) = 0$, i.e. they start and end with a constant slope.

The celebrated Holladay's Theorem states the special property of the splines which justifies their name and our choice. These functions are such that have minimal total curvature (assuming small curvatures), i.e. the result is as smooth as it can get. This property can be written as

$$\int_{\tilde{\varepsilon}_1}^{\tilde{\varepsilon}_n} \left[P''(E)\right]^2 dE \leq \int_{\tilde{\varepsilon}_1}^{\tilde{\varepsilon}_n} \left[f''(E)\right]^2 dE \tag{1}$$

for all interpolant twice continuously differentiable functions $f(E)$. The basic spline equation between two points is

$$P(E \in [E_i, E_{i+1}]) = P_i(E) = a_i + b_i(E - \tilde{E}_i) + c_i(E - \tilde{E}_i)^2 + d_i(E - \tilde{E}_i)^3 \tag{2}$$

Let

$$h_i = E_{i+1} - E_i \tag{3}$$

be the length of interval i. Then, property one above gives

$$a_i = \tilde{\sigma}_i \text{ for } i = 1, .., n \tag{4}$$

Property 2 above gives three conditions. The first one on the continuity of the second derivative of the function across segments

$$d_{i-1} = \frac{c_i - c_{i-1}}{3h_{i-1}} \tag{5}$$

The second one is the continuity of the function itself across segments

$$b_{i-1} = \frac{a_i - a_{i-1}}{h_{i-1}} - \frac{2c_{i-1} + c_i}{3} h_{i-1} \qquad (6)$$
$$\text{for } \; i = 1, .., n \text{ and with } \; |h_i| > 0$$

The third one is the continuity of the first derivative between segments, which upon substitution of the previous conditions yields

$$c_{i-1}h_{i-1} + 2\left(h_{i-1} + h_i\right)c_i + c_{i+1}h_i = \frac{a_{i+1} - a_i}{h_i/3} - \frac{a_i - a_{i-1}}{h_{i-1}/3} \qquad (7)$$
$$\text{for } \; i = 1, .., n \text{ and with } \; |h_i| > 0$$

The last property above defines the so-called *natural* splines, and gives the following conditions

$$c_1 = c_N = 0 \qquad (8)$$

Equations (7) are a tridiagonal system of $n-2$ equations which can be written in matrix notation as

$$\begin{bmatrix} 2\left(h_1 + h_2\right) & h_2 & & & \\ & \cdots & & & \\ & h_{i-1} & 2\left(h_{i-1} + h_i\right) & h_i & \\ & & \cdots & & \\ & & & h_{n-2} & 2\left(h_{n-2} + h_{n-1}\right) \end{bmatrix} \times$$
$$\times \begin{bmatrix} c_2 \\ \cdots \\ c_i \\ \cdots \\ c_{n-1} \end{bmatrix} = 3 \begin{bmatrix} \frac{a_3 - a_2}{h_2} - \frac{a_2 - a_1}{h_1} \\ \cdots \\ \frac{a_{i+1} - a_i}{h_i} - \frac{a_i - a_{i-1}}{h_{i-1}} \\ \cdots \\ \frac{a_n - a_{n-1}}{h_{n-1}} - \frac{a_{n-1} - a_{n-2}}{h_{n-2}} \end{bmatrix} \qquad (9)$$

and can be solved very efficiently even for large n values.

3 The Valanis-Landel hypothesis

The model uses an extension to transversely isotropic materials of the Valanis-Landel hypothesis. The Valanis-Landel hypothesis for isotropic materials states that the stored energy function $\bar{W}$ may be decomposed into the summation of three equal functions, each one having as argument a corresponding principal stretch:

$$\bar{W}(\lambda_1, \lambda_2, \lambda_3) = \sum_{i=1}^{3} \bar{\omega}\left(\lambda_i\right) = \bar{\omega}\left(\lambda_1\right) + \bar{\omega}\left(\lambda_2\right) + \bar{\omega}\left(\lambda_3\right) \qquad (10)$$

The existence of a unique function may be thought of as an intuitive extension to large strains of the one parameter G which governs the isotropic deviatoric behavior. This

assumption may be written in terms of principal logarithmic strains $E_i = \ln \lambda_i$ as

$$W(E_1, E_2, E_3) = \sum_{i=1}^{3} \omega(E_i) = \omega(E_1) + \omega(E_2) + \omega(E_3) \tag{11}$$

For transversely isotropic materials this decomposition is not valid because in general $W(\boldsymbol{E}) \neq W\left(\boldsymbol{Q}\boldsymbol{E}\boldsymbol{Q}^T\right)$ for an arbitrary rotation $\boldsymbol{Q}$. However, let us denote by $\boldsymbol{a} = \boldsymbol{e}_3$ the preferred direction, perpendicular to the isotropic plane. Then, it is possible to find a system of representation $\boldsymbol{X}_{pr}$ such that $E_{12} = E_{21} = 0$. In this system of representation

$$W(\boldsymbol{E}, \boldsymbol{a}) = W(E_1, E_2, E_3, E_{13}, E_{23}) \tag{12}$$

and the following necessary relationship for transversely isotropic materials is fulfilled

$$W(\boldsymbol{E}, \boldsymbol{a} \otimes \boldsymbol{a}) = W\left(\boldsymbol{Q}\boldsymbol{E}\boldsymbol{Q}^T, \boldsymbol{Q}\boldsymbol{a} \otimes \boldsymbol{a}\boldsymbol{Q}^T\right) \tag{13}$$

In view of Eq. (12), we can extend the Valanis-Landel hypothesis to transversely isotropic materials as

$$W(E_1, E_2, E_3, E_{13}, E_{23}) = \omega_1(E_1) + \omega_1(E_2) + \omega_3(E_3) + 2\omega_{13}(E_{13}) + 2\omega_{13}(E_{23}) \tag{14}$$

where we note now that there are 3 different strain energy functions. Since small strain transversely isotropic materials under isochoric behavior are governed by 3 independent constants, we may think of this expression as an intuitive extension to large strains.

4 Stress tensors

In isotropic incompressible elasticity the Cauchy, Kirchhoff and generalized Kirchhoff rotated stress tensors are coincident. In anisotropic elasticity the strain and stress tensors do not commute and, hence, it is necessary to distinguish between the different stress measures. Furthermore, the principal strain and stress directions are not necessarily coincident and none of them coincident with the principal material directions in orthotropy or transverse isotropy. Let $\boldsymbol{N}_i$ be the directions of principal stretches. Then, the relation between the rotated Kirchhoff stresses (or rotated Cauchy stresses) and the Generalized Kirchhoff stresses [18] are

$$T_{ij} = \frac{1}{2} \frac{\left(\lambda_j^2 - \lambda_i^2\right) / (\lambda_i \lambda_j)}{\ln \lambda_j - \ln \lambda_i} \bar{\tau}_{ij} \text{ for } i \neq j \tag{15}$$

Hence, proper conversion of stresses should be performed when matching experimental data.

5 The inversion formula

The experimental (or user prescribed) material data are fit using a piecewise cubic spline, as shown in Section 2. The stored elastic strain energy may not be directly obtained from these experimental data because, as we will see later, the relation between stored energy components of the Valanis-Landel decomposition and the stresses are of the type

$$\widetilde{\sigma}_i(\widetilde{E}_i) = \left.\frac{d\omega_i\left(E_i\right)}{dE_i}\right|_{\widetilde{E}_i} - \left.\frac{d\omega_i\left(E_i\right)}{dE_i}\right|_{a\widetilde{E}_i} \tag{16}$$

where $\tilde{\sigma}_i(\tilde{E}_i)$ are the experimental stresses $\tilde{\sigma}_i$ for given experimental strains $\tilde{E}_i$ in the i-direction and a is a constant such that $|a| < 1$. For the isotropic case, $a = -\frac{1}{2}$. Hence, it is imperative to obtain the $g\left(x\right)$ function such that for a given $f\left(x\right)$ function

$$f\left(x\right) = g\left(x\right) - g\left(ax\right) \tag{17}$$

where $f\left(0\right) = 0$. Then, the function $g\left(x\right)$ can be written in terms of the infinite but convergent series

$$g\left(x\right) = \sum_{k=0}^{\infty} f\left(a^k x\right) \tag{18}$$

To prove it, simply substitute (18) in (17) to obtain

$$\sum_{k=0}^{\infty} f\left(a^k x\right) - \sum_{k=0}^{\infty} f\left(a^{k+1} x\right) = f\left(x\right) + \underbrace{\sum_{k=1}^{\infty} f\left(a^k x\right) - \sum_{k=0}^{\infty} f\left(a^{k+1} x\right)}_{=0} = f\left(x\right) \tag{19}$$

However, sometimes it is necessary to relax the condition that a is constant. The reasons are that experimental data on $\tilde{E}_j(\tilde{E}_i)$ may not be considered linear or, in other cases, that a compatibility condition on the strain energy components is better fulfilled if nonlinear relations are assumed, see details in [18]. If a is not constant, then the inverse formula given above is not exact but the series are still convergent. In these cases, it can be shown that the error of the inversion formula is small and can be neglected for practical purposes [18].

6 Strain-energy function determination from experimental data

Using the concepts and formulations developed in previous sections, there exist different procedures to determine the stored-energy function (14) depending on the available set of measured data points. Next, we briefly explain the methodology we follow to obtain the first derivative of the unknown functions ω_1 and ω_3 when the available experimental measures are the tension-compression stress distributions $\widetilde{\sigma}_1(\widetilde{E}_1)$ and

$\widetilde{\sigma}_3(\widetilde{E}_3)$. The procedure to calculate ω'_{13} is common to all cases and can be followed in [18].

For a uniaxial test performed in any axis of $\boldsymbol{X}_{pr}$ we obtain

$$\bar{\boldsymbol{\sigma}} = \boldsymbol{T} = \frac{\partial W}{\partial \boldsymbol{E}} + p\boldsymbol{I} \tag{20}$$

with p representing a pressure-like quantity (hydrostatic pressure) required to maintain incompressibility. Then, in view of decomposition (14), we have

$$\bar{\sigma}_1 = \frac{d\omega_1\left(E_1\right)}{dE_1} + p; \qquad \bar{\sigma}_2 = \frac{d\omega_1\left(E_2\right)}{dE_2} + p; \qquad \bar{\sigma}_3 = \frac{d\omega_3\left(E_3\right)}{dE_3} + p \tag{21}$$

On the one hand, applying (21) for the uniaxial test in the isotropic direction $\boldsymbol{e}_1$, the pressure may be factored out from the equation in direction $\boldsymbol{e}_2$ and inserted in the other two equations to give

$$\widetilde{\sigma}_1(\widetilde{E}_1) = \left.\frac{d\omega_1\left(E_1\right)}{dE_1}\right|_{\widetilde{E}_1} - \left.\frac{d\omega_1\left(E_2\right)}{dE_2}\right|_{\widetilde{E}_2\left(\widetilde{E}_1\right)} \tag{22}$$

$$\left.\frac{d\omega_1\left(E_2\right)}{dE_2}\right|_{\widetilde{E}_2\left(\widetilde{E}_1\right)} = \left.\frac{d\omega_3\left(E_3\right)}{dE_3}\right|_{\widetilde{E}_3\left(\widetilde{E}_1\right)} \tag{23}$$

where the transverse strain distributions $\widetilde{E}_2(\widetilde{E}_1)$ and $\widetilde{E}_3(\widetilde{E}_1)$ are unknown. However, these variables are subjected to the incompressibility condition of the material, i.e., $\widetilde{E}_1 + \widetilde{E}_2(\widetilde{E}_1) + \widetilde{E}_3(\widetilde{E}_1) = 0$. Note that Equation (23) may be interpreted as a compatibility condition involving the derivative functions ω'_1 and ω'_3.

On the other hand, for the uniaxial test in the anisotropic direction $\boldsymbol{e}_3$, as a result of the transverse isotropy the equivalent compatibility equation to (23) is always identically fulfilled and only one equation has to be taken into account, namely:

$$\widetilde{\sigma}_3(\widetilde{E}_3) = \left.\frac{d\omega_3\left(E_3\right)}{dE_3}\right|_{\widetilde{E}_3} - \left.\frac{d\omega_1\left(E_1\right)}{dE_1}\right|_{-\frac{E_3}{2}} \tag{24}$$

where the relations $\widetilde{E}_1(\widetilde{E}_3) = \widetilde{E}_2(\widetilde{E}_3) = -\widetilde{E}_3/2$ have been used. Hence, the governing equations for this case are Equations (22), (23) and (24).

We first note that if we assume a linear behavior $\widetilde{E}_2(\widetilde{E}_1) = a\widetilde{E}_1$, the values $\omega'_1(\widetilde{E}_1)$ may be calculated with the inversion formula (18) for each experimental measure $\widetilde{E}_1$. Then, using the spline methodology given in Section 2, a piecewise spline function $\omega'_1(E_1)$ may be build. Secondly, the combination of Equations (23) and (24) results into another equation which may be solved by means of the inversion formula and it is possible to obtain the spline representation $\omega'_3(E_3)$. However, proceeding in that way, the spline functions have been calculated separately and Equation (23) will not be satisfied in general. Hence, the procedure lies in finding the value of the aforementioned parameter a which, after the calculation of the corresponding functions $\omega'_1(E_1)$ and $\omega'_3(E_3)$, provides the best fulfillment of relation (23). To achieve this, the least-squares method is a handy procedure. The value of a resulting from this analysis provides the best (approximated) solution of governing equations (22) to (24).

7 Examples

7.1 Incompressible isotropic hyperelastic materials

For isotropic materials, the Valanis-Landel assumption allows the modelling of the hyperelastic behavior in terms of a single scalar valued function ω of the principal logarithmic strains. Sussman & Bathe [16] illustrate how to obtain the derivative of this function by means of spline interpolations of the measured data points of a compression-tension uniaxial test. Their model is exactly recovered by our model when the initial tests correspond, effectively, to an isotropic material. In this case, $\omega_1 = \omega_3 = \omega$ and $E_2 = E_3 = -E_1/2$, so Equations (22) and (24) are the same equation and compatibility equation (23) is identically satisfied.

The two illustrative examples that Sussman & Bathe give in their paper are reproduced next using our model, taking as initial data the transversal strain distribution $E_2(E_1) = -E_1/2$ ($a = -1/2$).

In Figure (1.a), the following Cauchy stress distribution, defined in the strain range $-2 \leq E \leq 2$

$$\sigma(E) = \sigma_{nh}(E) + \sigma_p(E)$$

where

$$\sigma_{nh}(E) = \exp(2E) - \exp(-E)$$

$$\sigma_p(E) = \begin{cases} \sin^2(\pi E) & \text{if} \quad 0 \leq E \leq 1 \\ \\ 0 & \text{if} \quad -2 \leq E < 0 \quad \text{or} \quad 1 < E \leq 2 \end{cases}$$

has been represented using a large number of "experimental" points. $\sigma_{nh}(E)$ describes a small perturbation to the data, which is not well reproduced by the 9-term Ogden model. The interpolation of these data using splines (solid line) and the subsequently calculated stresses (dashed-line) show an exact agreement, even in the range $0 \leq E \leq 1$, as it occurred with the isotropic model.

In the second example, the following function, defined also in the strain range $-2 \leq E \leq 2$

$$\sigma(E) = 2\sinh(3E)(1 + 0.2\sin(10E)) + 2\sinh(1.5E)(1 - 0.2\sin(5E))$$

is considered. As explained in [16], the 3 and 9-term Ogden models do not fit correctly the waves produced by the trigonometric contributions. In Figure (1.b) it is shown that the transverse isotropic model gives exactly the same results as the Sussman-Bathe's isotropic model.

7.2 Incompressible transversely isotropic hyperelastic materials

Diani et al. present in their work [17] experimental data from uniaxial tensile tests for a transversely isotropic hyperelastic rubber-like material. The observed anisotropy is

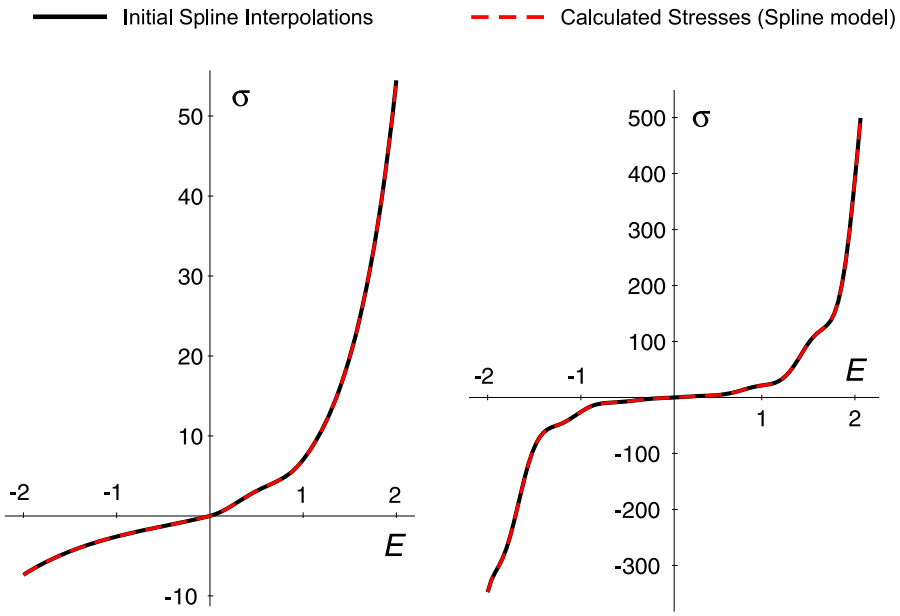

Figure 1: Examples 1 (a - Left) and 2 (b - Right) – Initial piecewise spline interpolations of assumed data $\widetilde{\sigma}(\widetilde{E})$ from uniaxial tests performed on an isotropic material — Calculated stresses using the transversely isotropic spline-based model with a initial distribution $\widetilde{E}_2(\widetilde{E}_1) = -\widetilde{E}_1/2$. No difference is observed between both lines.

of about 30% (stress) for a stretch ratio of 150%. The mentioned measured data points are shown as dots in Figure 2.

As can be observed, the stresses calculated by application of the procedure explained in Section 6 reproduce very accurately the experimental measures in both directions. The experimental data by Diani et al. are given in terms of stretches (λ_i) and first Piola-Kirchhoff stresses (P_i) and hence the proper conversion has been previously performed ($E_i = \ln \lambda_i$; $\sigma_i = P_i \lambda_i$). Furthermore, since only uniaxial tension measures are provided, the stress distribution $\sigma(E)$ has been regarded as an odd function of the strains in order to be able to apply the inversion formula. If compression measures had been available, they should have been employed.

8 Conclusion

In this work we have extended the Sussman-Bathe splines model originally developed for isotropic hyperelasticity to transversely isotropic materials. As shown, the model converges to the Sussman-Bathe model for the case of isotropy. Predictions for the transversely isotropic rubber-like hyperelastic material tested by Diani et al. are also given. It is seen that very accurate predictions are obtained.

The procedure presents an attractive option for constitutive behavior modelling in the finite element context since the user has to simply supply some stress-strain data

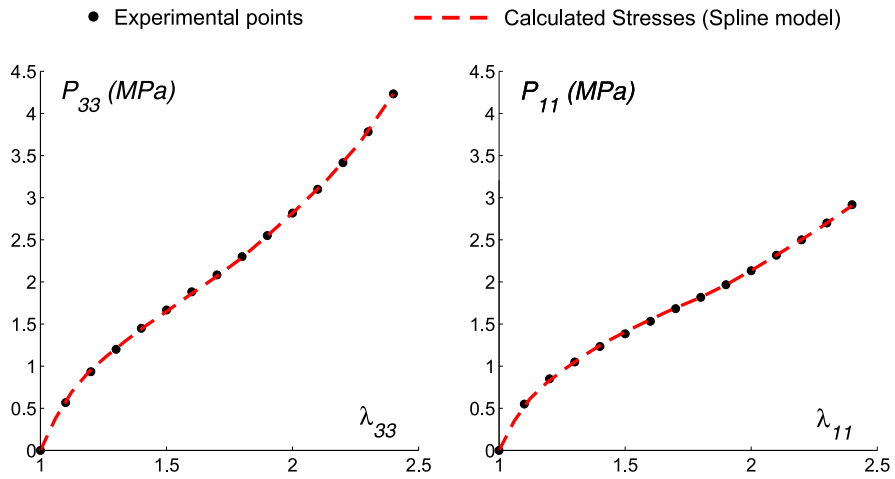

Figure 2: Measured nominal tension points $\widetilde{P}_3(\widetilde{\lambda}_3)$ and $\widetilde{P}_1(\widetilde{\lambda}_1)$ from uniaxial tests on calendered rubber in the anisotropic and transverse directions (Diani et al. [17]) — Calculated stresses using the transversely isotropic spline model.

and the formulation is able to closely predict such behavior without sacrificing physical and mathematical correctness. The model is applicable to a large amount of important materials as one fiber composites, living tissues and some polymers.

Acknowledgements

Financial support for this work has been given by the Dirección General de Proyectos de Investigación of the Ministerio de Ciencia e Innovación and the Ministerio de Economía y Competitividad of Spain under grants DPI2008-05423 and DPI2011-26635

References

[1] R.M. Jones, "Mechanics of composite materials", New York, Taylor and Francis, 1999.

[2] Y. Zhou, R. Zheng, "Dynamic response of elastic layer on transversely isotropic saturated soil to train load", Rock and Soil Mechanics, 2011.

[3] G. Raumann, "The anisotropy of the elastic constants of transversely isotropic polyethylene terephthalate", British Journal of Applied Physics, 14, 795, 1963.

[4] J.A. Weiss, B.N. Maker, S. Govindjee, "Finite element implementation of incompressible, transversely isotropic hyperelasticity", Computer Methods in Applied Mechanics and Engineering, 135, 107-128, 1996.

[5] R. Huiskes, "On the modelling of long bones in structural analyses", Journal of Biomechanics, 15, 65-69, 1982.

[6] G.A. Holzapfel, R.W. Ogden, "Constitutive modelling of passive myocardium: a structurally based framework for material characterization", Phil. Trans. R. Soc. A, 367, 3445-3475, 2009.
[7] C.J. Choung, Y.C. Fung, "Residual stress in arteries", Frontiers in Biomechanics, Springer-Verlag, New York, 117-179, 1986.
[8] G. Limberta, J. Middletona, "A transversely isotropic viscohyperelastic material: Application to the modeling of biological soft connective tissues", International Journal of Solids and Structures, 41, 4237-4260, 2004.
[9] R.W. Ogden, "Large deformation isotropic elasticity: on the correlation of theory and experiment for incompressible rubberlike solids", Proceedings of the Royal Society London Series A, 326, 565-584, 1972.
[10] M. Mooney, "A theory of large elastic deformation", Journal of Applied Physics, 11, 582-592, 1940.
[11] R.S. Rivlin, "Large Elastic Deformations of Isotropic Materials. IV. Further Developments of the General Theory", Phil. Trans. R. Soc. Lond. A, 241, 835, 379-397, 1948.
[12] P.J. Blatz, W.L.Ko, "Application of finite elasticity theory to the deformation of rubbery materials", Transactions of the Society of Rheology, 6, 223-251, 1962.
[13] E.M. Arruda, M.C. Boyce "A three-dimensional constitutive model for the large stretch behavior of rubber elastic materials", Journal of the Mechanics and Physics of Solids, 41, 389-412, 1993.
[14] M. Itskov, N. Aksel, "A class of orthotropic and transversely isotropic hyperelastic constitutive models based on a polyconvex strain energy function", International Journal of Solids and Structures, 41, 3833-3848, 2004.
[15] G.A. Holzapfel, T.C. Gasser, R.W. Ogden, "A New Constitutive Framework for Arterial Wall Mechanics and a Comparative Study of Material Models", Journal of Elasticity, 61, 1-48, 2000.
[16] T. Sussman, K.J. Bathe, "A Model of Incompressible Isotropic Hyperelastic Material Behavior using Spline Interpolations of Tension-Compression Test Data", Communications in Numerical Methods in Engineering, 25, 53-63, 2009.
[17] J. Diani, M. Brieu, J.M. Vacherand, A. Rezgui, "Directional model for isotropic and anisotropic hyperelastic rubber-like materials", Mechanics of Materials, 36, 313-321, 2004.
[18] M. Latorre, F.J. Montáns, "Extension of the Sussman-Bathe spline-based hyperelastic model to incompressible transversely isotropic materials", to appear.